Chemical Science

Accepted Manuscript

This article can be cited before page numbers have been issued, to do this please use: W. feng, M. Si, K. Cao, W. Lu, X. Zhang and T. Chen, *Chem. Sci.*, 2026, DOI: 10.1039/D5SC08423G.

ROYAL SOCIETY OF CHEMISTRY

rsc.li/chemical-science

Confining chromophores by polymer conformation rigidification for room-temperature phosphorescence hydrogels

Received 00th January 20xx,
Accepted 00th January 20xx

DOI: 10.1039/x0xx00000x

Weihao Feng,[ab] Muqing Si,[ab] Kuangzheng Cao,[c] Wei Lu,*[ab] Xiaoye Zhang*[ab] and Tao Chen*[ab]

Organic room-temperature phosphorescent (RTP) materials have played an important role in many emerging photonic applications, such as flexible electronics, bioimaging, and information anti-counterfeiting encryption, due to their excellent properties of large Stokes shift and long lifetime. However, RTP emission of polymer materials requires the restriction of rigid chemical environment, which greatly limits their applications in dry state that usually have poor stretchability. Polymeric RTP hydrogels offer excellent soft wet feature and tunable mechanical properties, providing an ideal solution to address the above challenge. Various preparation strategies have been developed to achieve RTP emission by confining chromophores through polymer conformation rigidification, such as physical doping, chemical grafting, and supramolecular polymerization. This review aims to systematically summarize recent progress in this young but flourishing research area. Subsequently, the application fields of polymeric RTP hydrogels are briefly reviewed. The current challenges and future outlooks of this field are also discussed to attract new interest and inspire more efforts.

1. Introduction

Organic room-temperature phosphorescence (RTP) materials are photoluminescent materials with long emission lifetimes.[1-6] The RTP emission can persist after the excitation light stops. Due to its excellent merits of large Stokes shift and long lifetime, RTP materials play an important role in many emerging photonic applications, such as flexible electronics,[7-10] bioimaging,[11-14] and information anti-counterfeiting encryption[15-18]. The generation of RTP requires electrons to overcome the spin prohibition and realize the intersystem crossing of singlet and triplet states. However, triplet excitons are easily quenched by oxygen or return to the ground state through non-radiative transitions.[19-20] Therefore, in order to achieve RTP emission, strategies such as host-guest interactions,[21-22] metal-organic frameworks (MOFs),[23-24] and crystals[25-26] are commonly employed to confine the chromophores in a dry and rigid chemical environment. These approaches reduce the non-radiative decay process of the triplet state caused by the movement and collision of phosphorescence molecules and the quenching of the triplet excitons by oxygen, and achieve RTP emission. Therefore, most traditional RTP materials often have the shortcomings of poor biocompatibility and flexibility, which greatly limits their promotion in practical applications.[27-28] The development of flexible and soft RTP materials has attracted great interest.

Polymeric hydrogels, which usually exist as highly water-swollen quasi-solids and combine many advantages of both the solution and solid states, have excellent biocompatibility and tunable mechanical properties.[29-34] Combining the superior properties of RTP materials with hydrogels to construct polymeric RTP hydrogels provides an ideal solution to the above challenges. Polymeric RTP hydrogels exhibit outstanding flexibility and processability, which enable them to adapt to complex surfaces for applications in wearable devices, flexible sensors and soft robots. Meanwhile, the hydrogels network can respond to external stimuli (such as pH, temperature, and specific molecules), resulting in changes in volume or conformation, and then manipulating the RTP emission. This property provides a new strategy for information anti-counterfeiting. In addition, compared with many traditional RTP materials with poor biocompatibility and difficulty in aqueous dispersion, polymeric RTP hydrogels have broad application prospects in the field of bioimaging. Consequently, polymeric RTP hydrogels have numerous irreplaceable advantages over conventional rigid RTP materials. However, polymeric RTP hydrogels are highly sensitive to environmental conditions and easily quenched. The swelling of polymer networks and hydration effect of molecular fragments inevitably enhance polymer chain flexibility, resulting in significant increase of fast nonradiative decay (k_{nr}) or oxygen quenching (k_q).[35] The core idea to solve the above problems is to provide a rigid microenvironment for chromophores in the hydrogels. Rigid microenvironment refers to the rigidification of the chemical environment around the chromophores, including molecular-scale (e.g., hydrogen bonds, host-guest interactions, and coordination bonds) or larger-scale (e.g., crystallization and phase separation) interactions. The construction of a rigid microenvironment can stabilize triplet excitons, inhibit non-radiative transitions, and thereby achieve RTP emission. [36-43]

So far, although the research on polymeric RTP hydrogels is still in infancy, a number of excellent studies have been

[a] State Key Laboratory of Advanced Marine Materials, Zhejiang Key Laboratory of Extreme-environmental Material Surfaces and Interfaces, Ningbo Institute of Materials Technology and Engineering, Chinese Academy of Sciences, Ningbo 315201, China E-mail: luwei@nimte.ac.cn; zhangxiaoye@ nimte.ac.cn; tao.chen@nimte.ac.cn
[b] School of Chemical Sciences, University of Chinese Academy of Sciences, 19A Yuquan Road, Beijing 100049, China
[c] Department of Digital Technologies, Hainan Bielefeld University of Applied Sciences, Danzhou 571700, China

View Article Online
DOI: 10.1039/D5SC08423G

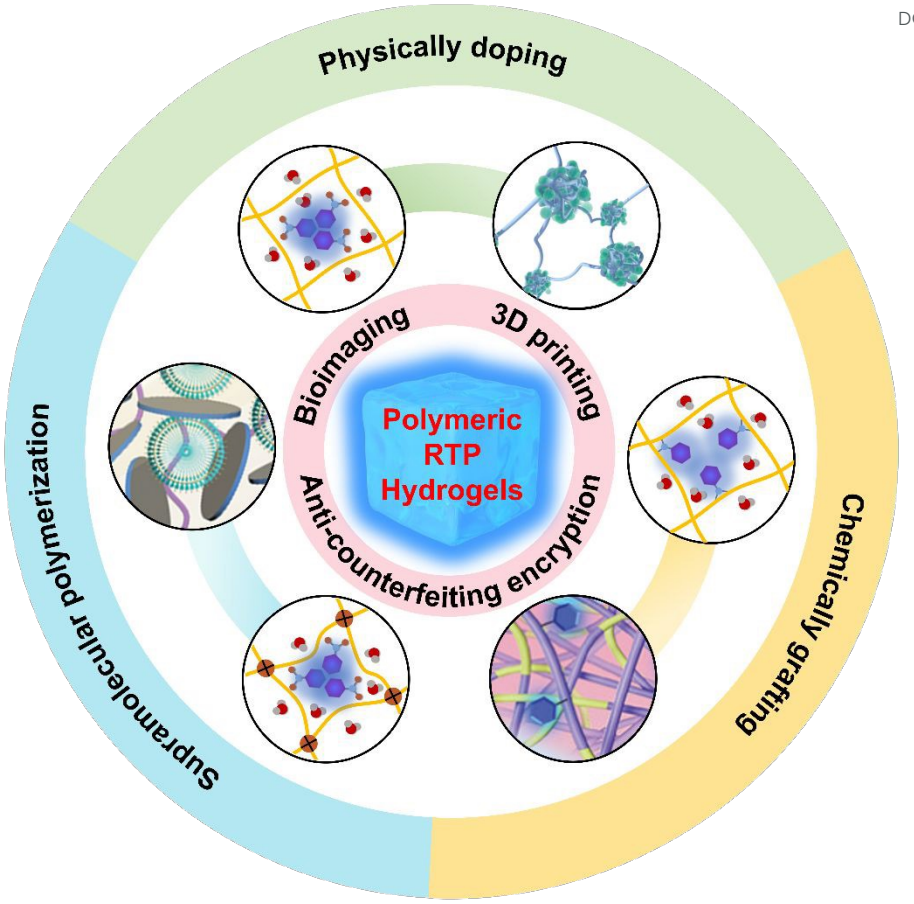

Scheme 1 Synthetic strategy of polymeric RTP hydrogels and their applications in numerous frontier fields.

reported. While a review has summarized RTP hydrogels from the perspective of chromophore types,[44] no review has examined RTP hydrogels from the standpoint of preparation strategies. This review aims to systematically outline the construction of polymer RTP hydrogels and their RTP properties. Polymeric RTP hydrogels are primarily classified based on fabrication strategy, including physical doping, chemical grafting and supramolecular polymerization of hydrogels (Scheme 1). Subsequently, a brief introduction is provided to the various potential applications of polymeric RTP hydrogels, including three-dimensional (3D) printing, bioimaging and anti-counterfeiting encryption. Finally, the future challenges and prospects are also discussed. This review is likely to attract widespread attention from interdisciplinary researchers, providing theoretical guidance and innovative insights for the design and application of next- generation smart materials.

2. Mechanistic Insights

2.1 Fundamental Mechanism of Room-Temperature Phosphorescence (RTP)

Room-temperature phosphorescence (RTP) arises from a process in which molecules, upon excitation, undergo intersystem crossing (ISC) to reach the triplet state, and then slowly radiate light.[45] The key challenge is that excitons in the delicate triplet state are highly prone to losing energy through non-radiative transitions, such as vibrational and rotational motions, at room temperature, leading to phosphorescence quenching. Therefore, suppressing non-radiative transitions is essential for achieving efficient RTP. The question then becomes: How can we create such a rigid microenvironment in soft, water-rich hydrogels?

2.2 The Crucial Role of Rigid Microenvironments in RTP

Although hydrogels are macroscopically soft, their crosslinked network structure at the microscopic level provides effective spatial confinement, or a rigid microenvironment, which is a decisive factor in suppressing non-radiative transitions and regulating RTP lifetime (τ). The crosslinking density of the polymer network influences the RTP intensity of the hydrogel. Studies show that as the polymerization time increases, the RTP intensity gradually improves.[46] The water content is also an important factor influencing RTP performance. Compared to polymer networks with high water content, those with low water content have more densely packed polymer chains, blocking oxygen pathways, and significantly enhancing RTP. Furthermore, introducing rigid segments is a key method to improve RTP. For example, the crystallization within a polyvinyl alcohol (PVA) gel network increases rigidity, reducing the mobility of chromophore molecules and enhancing RTP performance.[47] The incorporation of rigid nanoparticles as multifunctional crosslinking points not only improves mechanical properties but also creates more restricted “rigid nanodomains” that help stabilize the triplet excitons.[48]

View Article Online
DOI: 10.1039/D5SC08423G

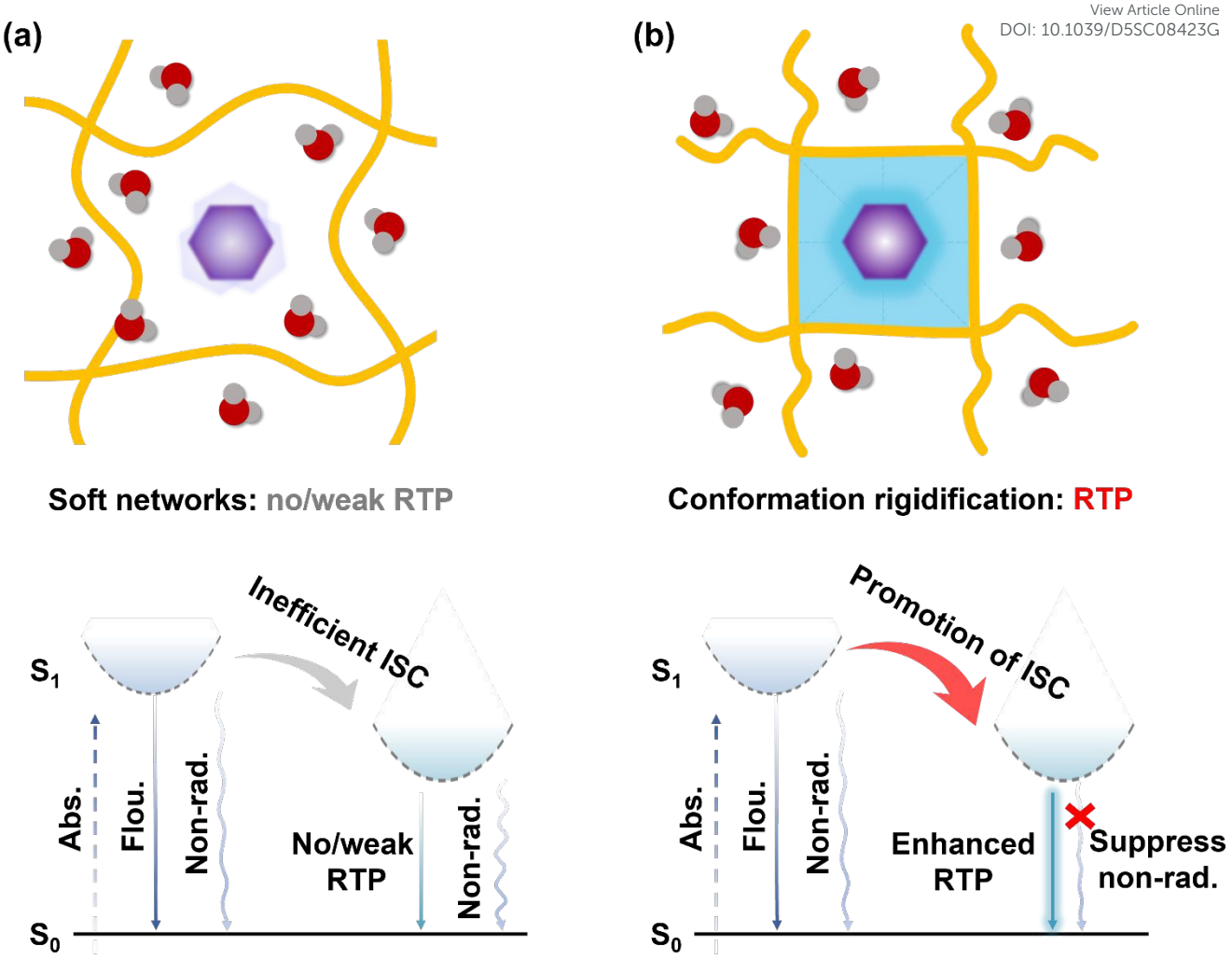

Fig. 1 Mechanism of polymeric RTP hydrogels. Schematic Jablonski illustration depicts luminescence mechanisms in a) soft networks and b) rigid microenvironments.

In addition to the adjustment of the polymer network, the interactions between the polymer matrix and chromophore also affect RTP performance. For instance, hydrogen bonds between the molecules and the side-chain amides can not only limit the mobility of the chromophore but may also alter its electronic structure, facilitating the ISC process. The spatial confinement of chromophore molecules in an ultra-entangled polymer network, induced by hydrogen bonding, results in ultralong room-temperature phosphorescence. Moreover, some dynamic crosslinked hydrogels may exhibit reversible changes in RTP performance in response to external stimuli. In summary, this strategy of creating a "rigid microenvironment within a soft matrix" establishes the conditions necessary to stabilize triplet excitons within the macroscopic softness of hydrogels. This forms the foundation for achieving long-lived, high-intensity RTP.

3. Construction strategy of polymeric RTP hydrogels

3.1 Physical doping chromophores into polymeric hydrogels

Physical doping is the simplest and most direct method for creating polymeric RTP hydrogels. However, phosphorescent chromophores are highly sensitive to the abundant water and dissolved oxygen in hydrogels, readily leading to non-radiative transitions and quenching of triplet excitons. Therefore, chromophores are often protected by encapsulating them within nanoparticles or by utilizing their interactions with polymer matrices.

The formation of stable nanoparticles through assembly represents an effective method for preparing RTP hydrogels. In 2022, He *et al.* proposed a strategy for the preparation of polymeric RTP hydrogels by boric acid (BA)-doped silicon nanoparticles (BSiNPs). (3-Aminopropyl)trimethoxysilane (APTMS) was reacted with trisodium citrate under microwave irradiation to produce silicon-based nanoparticles (SiNPs), which exhibited blue fluorescence emission. BAs were subsequently doped into the SiNPs system. The glassy-state BSiNPs were formed after the high-temperature and pressure reaction (Fig. 2a).[48] The encapsulated glass-state BSiNPs were able to stabilize triplet excitons and reduce non-radiative transitions. The RTP properties were effectively enhanced. As shown in Fig. 2b, the BSiNPs were uniformly dispersed in the polyvinyl alcohol (PVA) hydrogels. And they exhibited ultra-long afterglow up to 20 s (Fig. 2c).

View Article Online
DOI: 10.1039/D5SC00425G

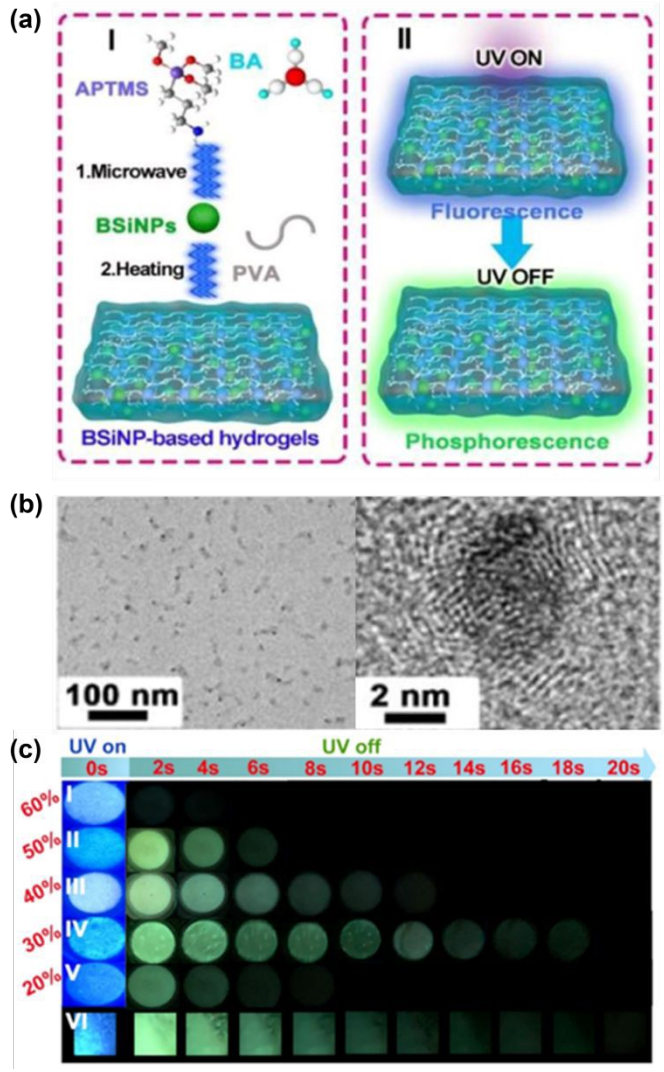

Fig. 2 Physically doping chromophores into polymeric RTP hydrogels. (a) Synthesis of boron-doped silicon nanoparticles (BSiNPs) and BSiNP-based RTP hydrogels under microwave irradiation. (b)Transmission Electron Microscope (TEM)images of the BSiNPs. (c) RTP photos of the BSiNPs with different Si/Si + B (mol %) values and the hydrogels.

Nanocarbon dots are also a type of material that enables long-lived phosphorescence. In 2024, Liu *et al.* developed a strategy to achieve phosphorescence emission in hydrogels by encapsulating carbon nanodots (CNDs) within a silica shell, thereby shielding them from water and oxygen. The polymeric RTP hydrogels were then fabricated through in situ polymerization with acrylic acid (AA), C=C bond modified β-cyclodextrin (β-CD-DA) and adamantane (Ad-DA) (Fig. 3a).[49] As shown in Fig. 3b, the CNDs@silica were uniformly dispersed in the hydrogels. The CNDs@silica provided long-lived green phosphorescence, and the polymeric RTP hydrogels exhibited an ultra-long lifetime of up to 1261 ms (Fig. 3c). β-CD-DA and Ad-DA confer more than 30 times the stretchability to the hydrogels through host-guest interactions (Fig. 3d). Furthermore, the hydrogel was able to efficiently transfer energy to the fluorescence dyes Rhodamine B and Eosin Y through efficient TS-FRET, resulting in long-lived red and yellow delayed fluorescence (Fig. 3a).

Beyond encapsulating phosphorescent chromophores to shield them from water and oxygen, leveraging physical interactions between chromophores and polymer matrices offers a more universal and direct approach to forming physically doped RTP hydrogels. For example, the hydrogen bonding between the chromophores and the polymeric chains can effectively achieve RTP emission. In 2025, Wang *et al.* developed a polymeric RTP hydrogels construction method based on strong hydrogen bonding interactions between nonconventional chromophores (NCCs) and polymeric chains (Fig. 4a).[50] Biuret (BIU), polyvinyl alcohol (PVA), and polymaleic acid (PMAc) were dissolved in glycerol/water mixed solvent and formed organohydrogels (PVA/BIU/PMAc) through freeze-thawing treatment. The strong hydrogen bonds between NCCs and the polymer chains suppress non-radiative transitions and promote the aggregation of NCCs, thereby stiffening molecular conformations and forming spatial conjugation. The RTP hydrogels exhibited the RTP lifetime of up to 782.8 ms (Fig. 4b). Furthermore, the hydrogels demonstrated significant excitation-dependent RTP emission. Remarkably, the hydrogels' RTP emission wavelength varies with the change in the excitation wavelength (Fig. 4c).

By forming hydrogen bond interactions between the polymer chains and chromophores, not only can polymeric RTP hydrogels be constructed, but the hydrogels are also endowed with excellent mechanical properties. Chen *et al.* in 2024 developed a high-strength polymeric RTP hydrogels (W-hydrogels) by the in-situ polymerization of acrylamide (AAm) in the presence of delignified wood. This strategy was to form molecular clusters through hydrogen bond interactions between lignin and acrylamide (Fig. 4d).[51] Such enhanced interactions facilitate the confinement of lignin and trigger the radiative migration of triplet excitons, thus enabling RTP emission. The hydrogels exhibited RTP emission at around 490 nm and gave out obvious green luminescence after removing the UV light (Fig. 4e). As a result of the molecular interactions between the components of delignified wood and polyacrylamide (PAAm), the W-hydrogels exhibited extremely high tensile strength. Moreover, the tensile strength of W-hydrogel treated with ethanol increased significantly, and the whole process was reversible (Fig. 4f). The reversibility of this process enables the RPT hydrogel material to be applied in a wider range of scenarios.

These chromophores interact with polymer chains to form a super-entangled state, enabling the hydrogel to effectively achieve phosphorescent emission and super-stretch properties. In 2025, Chen *et al.* incorporated 4-diphenylboronic acid@β-Cyclodextrin (4-BB@β-CD) into a poly(2-(acryloxy)ethyl trimethylammonium chloride) (PAETC) network to prepare an ultra-stretchable polymer RTP hydrogel. Under water-limiting conditions, the PAETC chain forms a hyper-entangled structure and synergistically densify the 4-BB@β-CD aggregates through supramolecular confinement, effectively suppressing molecular vibrations and stabilizing triplet states (Fig. 5a).[52] Impressively, the hydrogels exhibit intense RTP emission at around 500 nm and ultralong lifetime up to 970.7 ms under room conditions (Fig. 5b, c). Crucially, the entanglement-dominated physical network free of static chemical crosslinking enables continuing chain disentanglement during stretching for efficient energy dissipation, achieving excellent uniaxial/biaxial (21000%/10000%) stretchability (Fig. 5d, e). Notably, these PAETC/4-BB@β-CD hydrogels still maintained bright and long-lived RTP under various strains (Fig. 5e).

All these impressive recent advancements suggest that excellent and multi-functional RTP properties can be imparted to hydrogel materials through simple physical doping as well as material design.

3.2 Chemical grafting chromophores into polymeric hydrogels

While the physical doping method is simple, the problem of phosphorescence small-molecule leakage significantly limits the long-term stability and practical applications of polymeric RTP hydrogels. To fundamentally address this problem, researchers

View Article Online
DOI: 10.1039/D5SC08423G

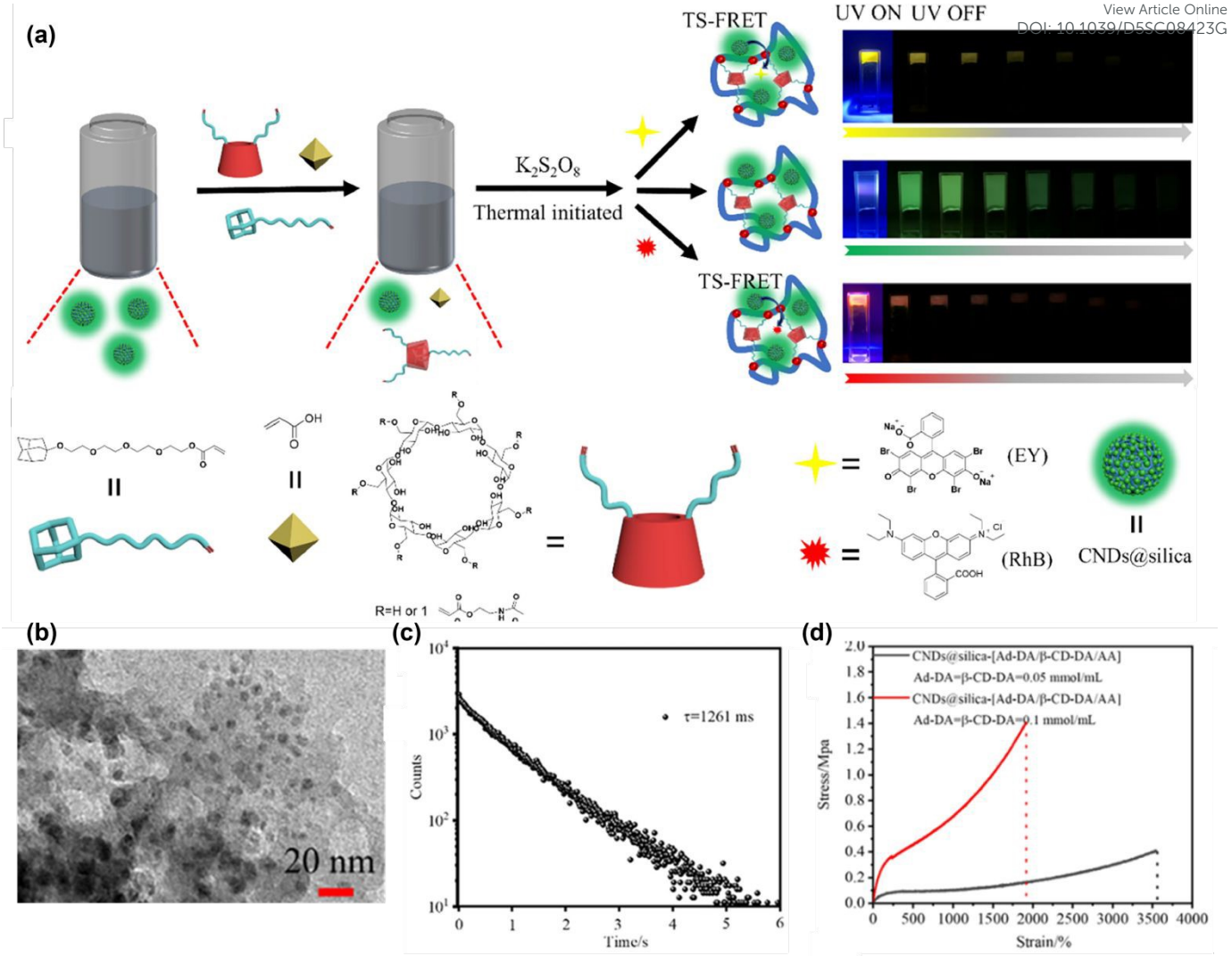

Fig. 3 Physically doping chromophores into polymeric RTP hydrogels. (a) Construction of CNDs@silica-(Ad-DA/β-CD-DA/AA) hydrogels and the green RTP and delay fluorescence photos of hydrogels. (b) TEM images of CNDs@silica. (c) Lifetime decay curve of the hydrogel collected at 520 nm. (f) Tensile stress-strain curves of hydrogels with different concentrations of Ad-DA/β-CD-DA assembly.

have covalently grafted the chromophores onto the three-dimensional network of the hydrogels. Due to the stability of covalent bonds, grafting chromophores onto polymer chains enhance the stability of luminescence intensity and lifetime.[51] The interactions between the polymeric networks provide a highly rigid microenvironment for the phosphorescence chromophores, effectively stabilizing triplet excitons and suppressing non-radiative transitions, ultimately facilitating the construction of polymer RTP hydrogels.

For example, the formation of rigid microenvironment through host-guest interactions can effectively prepare polymeric RTP hydrogels by grafting host and guest molecules onto the polymeric main chain. In 2014, Tian *et al.* grafted β-cyclodextrin (β-CD) and α-bromonaphthalene (α-BrNp) onto the polymeric main chain (Fig. 6a).[53] The host-guest recognition between β-CD and α-BrNp enabled hydrogels formation without the need for additional crosslinking. The rigid microenvironment provided by the host-guest interactions successfully achieved RTP emission and exhibited the lifetime of 0.56 ms. At the same time, the hydrogels exhibited excellent self-healing properties (Fig. 6b). Similarly, in 2016, they achieved RTP emission in hydrogels with the lifetime of 0.32 ms by using different host molecule γ-cyclodextrin (γ-CD) and guest molecule 4-bromo-1,8-naphthalic anhydride (BrNpA) (Fig. 6c).[54]

By designing the molecular structure and multi-functionalization of phosphorescence molecules, which can construct rigid microenvironment in hydrogels. In 2024, He *et al.* developed a novel multi-functional molecule based on benzothiadiazole-based dialkene (BTD-HEA), which serves as a phosphorescence emitter, initiator, and crosslinker in polymeric RTP hydrogels. BTD-HEA exhibits a high triplet exciton generation ability and a dialkene structure, enabling it to effectively initiate the polymerization of acrylamide-based monomers while acting as a crosslinking site to form a crosslinked network structure (Fig. 7a).[46] Additionally, the hydrogels' distinct fluorescent-phosphorescent colorimetric characteristics offer a more sensitive approach for visually monitoring the polymerization process (Fig. 7b). The RTP intensity and rheological tests demonstrate that the crosslinking degree of the hydrogel network increases with polymerization time (Fig. 7c, d). Consequently, the thermal motion of BTD-HEA was restricted, and non-radiative transitions were suppressed, leading to changes in the RTP emission. By utilizing BTD-HEA as a photoinitiator, various shapes of polyhydroxyethyl acrylate (PHEA)

hydrogels can be prepared through 3D printing. Moreover, the hydrogel retains a purple

View Article Online
DOI: 10.1039/D5SC08423G

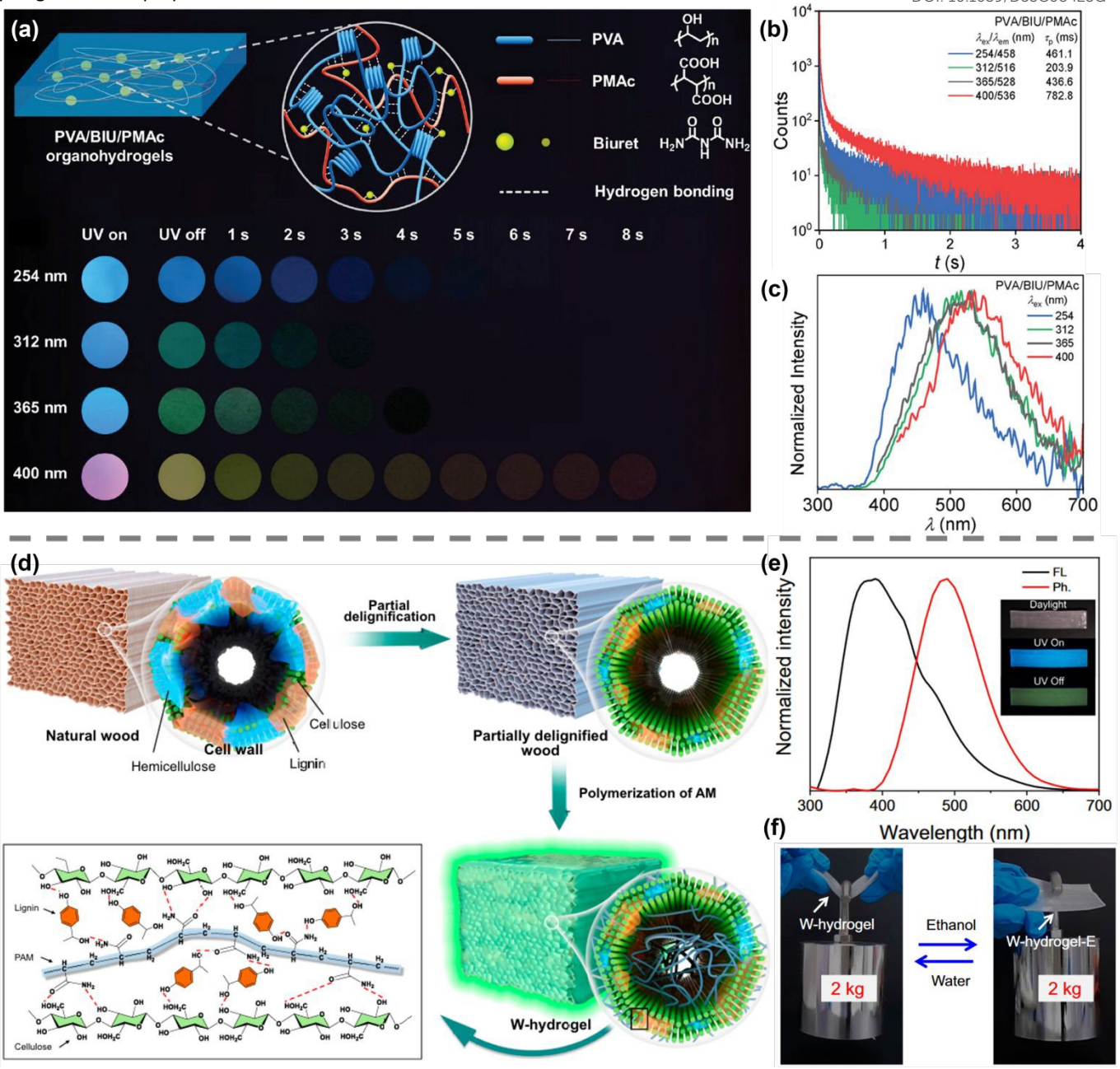

Fig. 4 Physically doping chromophores into polymeric RTP hydrogels. (a) The schematic illustration of the crosslinking mechanism in PVA/BIU/PMAc organohydrogels and RTP photos of hydrogels after ceasing irradiations of different wavelengths. (b-c) Phosphorescence lifetime profiles and delayed emission spectra of PVA/BIU/PMAc organohydrogels. (d) Schematic illustration of the preparation of RTP W-hydrogel from natural wood. (e) Fluorescence (black line) and phosphorescence spectra (red line) of W-hydrogel upon excitation of 290 nm. Inset: Photos of W-hydrogel under visible light, under UV light and after removing UV light. (f) Photos of W-hydrogel and W-hydrogel-E loaded with a weight.

afterglow even after the cessation of 365 nm UV excitation (Fig. 7e). Although purple afterglow is uncommon, its long-lasting luminescence characteristics confirm its RTP emission.

The formation of phase-separated structure in hydrogels can also achieve the construction of rigid microenvironment. In 2024, Lü *et al*. induced in situ phase separation in hydrogels via acid treatment, successfully preparing polymeric RTP hydrogels. Initially, the researchers prepared hydrogels by copolymerizing AAm and N-(4-(9H-carbazole-9-yl)phenyl)-2-acrylamide chromophore (CzPA). The hydrogels were then immersed in a hydrochloric acid aqueous to hydrolyze the amide groups in the hydrogels. The interaction between amide and carboxylic acids groups formed dense hydrogen bonds, leading to phase separation. This process resulted in the formation of a tight network structure that restricted the motion of chromophores and suppressed non-radiative transitions (Fig. 7f).[55] The hydrogels

displayed excellent stability in water, showing minimal change over thirty days, with consistent RTP intensity and afterglow (Fig. 7g, h). Mechanical properties play a very important role in expanding the application range of polymeric RTP hydrogels and extending the service life of materials. However, the emission of RTP requires the suppression of non-radiative transitions, which is contradictory to the softness, high water content, and stretchable properties of hydrogels. Therefore, it is necessary to construct a local rigid microenvironment in the hydrogels. The construction of rigid microenvironments does not compromise the overall mechanical properties of the hydrogel, so the polymeric RTP hydrogels have the advantage of widely adjustable mechanical properties. In addition to the excellent RTP properties, this polymeric RTP hydrogels also have excellent and widely tunable mechanical properties. In a series of hydrogels with different H-treatment times, the hydrogel with H-treatment 6 h has a fracture strain of nearly 1000%, and the hydrogel with H-treatment 14 h has a fracture stress of more than 11 MPa.

In addition to introducing typical chromophores, RTP emission can also be achieved by the aggregation and confinement of

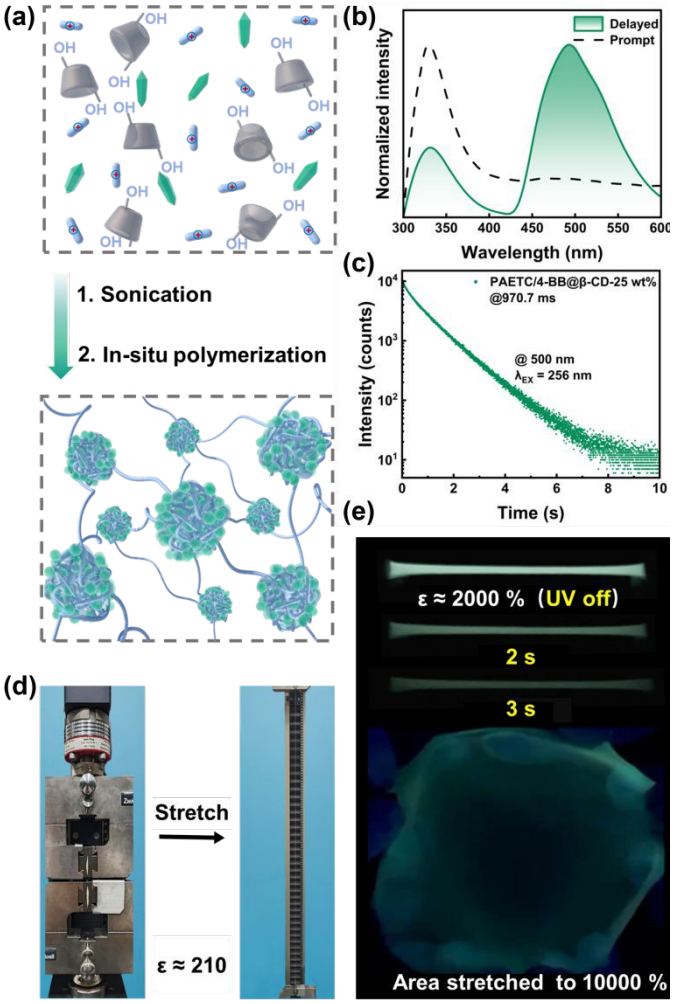

Fig. 5 Physically doping chromophores into polymeric RTP hydrogels. (a) Illustration showing the synthetic procedure of PAETC/4-BB@β-CD hydrogels. (b) Normalized delayed and prompt luminescence spectrum of the PAETC/4-BB@β-CD hydrogels. (c) Time-resolved emission-decay test of the PAETC/4-BB@β-CD-25 wt% hydrogel recorded at 500 nm. (d) Photos of the PAETC/4-BB@β-CD-25 wt% hydrogel after being stretched to 21000%. (e) Photos of the PAETC/4-BB@β-CD-25 wt% hydrogel after uniaxial stretching to 2000% and biaxial stretching to an area strain of 10000% after removing the UV light.

electron-rich groups, such as carbonyl groups. In 2024, Wu *et al.* proposed a strategy for the preparation of polymeric RTP hydrogels through polymerization-induced crystallization (Fig. 8a).[56] The strategy exploited the solubility difference of crown ethers (CEs) in monomer and polymer states. During the polymerization process, the solubility of the CEs sharply decreases, leading to the formation of large spherulites that compress and confine the polyacrylamide hydrogel matrix. The approach leads to the formation and aggregation of carbonyl group clusters, thereby achieving RTP emission. The hydrogels exhibit excellent stretchability and resilience, with visible afterglow (Fig. 8b).

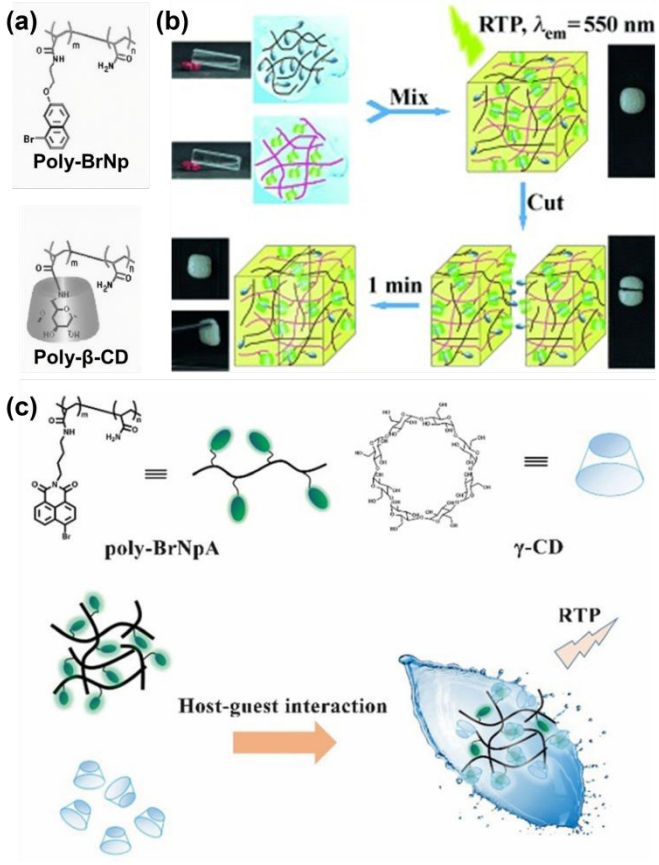

Fig. 6 Chemical grafting chromophores into polymeric RTP hydrogels. (a) Structures of host polymer poly-b-CD and guest polymers poly-BrNp. (b) Preparation of the poly-α-BrNp/poly-β-CD hydrogels and self-healing processes. (c) Schematic representation of the polymeric RTP hydrogel via host-guest interaction between poly-BrNpA and γ-CD.

Building on the above research findings, in 2024, Wu *et al.* further achieved control of spherulites structure in the hydrogels by modulating the hydrogel network stiffness. The stiffness of the PAAm network was precisely adjusted by regulating the concentrations of photoinitiator and chemical crosslinking agents, as well as the intensity of UV light. Regular spherulites are formed in relatively stiff hydrogels, whereas banded spherulites with twisted crystal fibers are obtained in hydrogels (Fig. 8c).[57] The structure of the spherulites can be directly observed through polarized optical microscope (Fig. 8d, f). The formation of twisted

View Article Online
DOI: 10.1039/D5SC08423G

crystalline fibers was linked to the dynamic changes in crystallization pressure and network impedance. Hydrogels with regular spherulites exhibited stronger fluorescence and

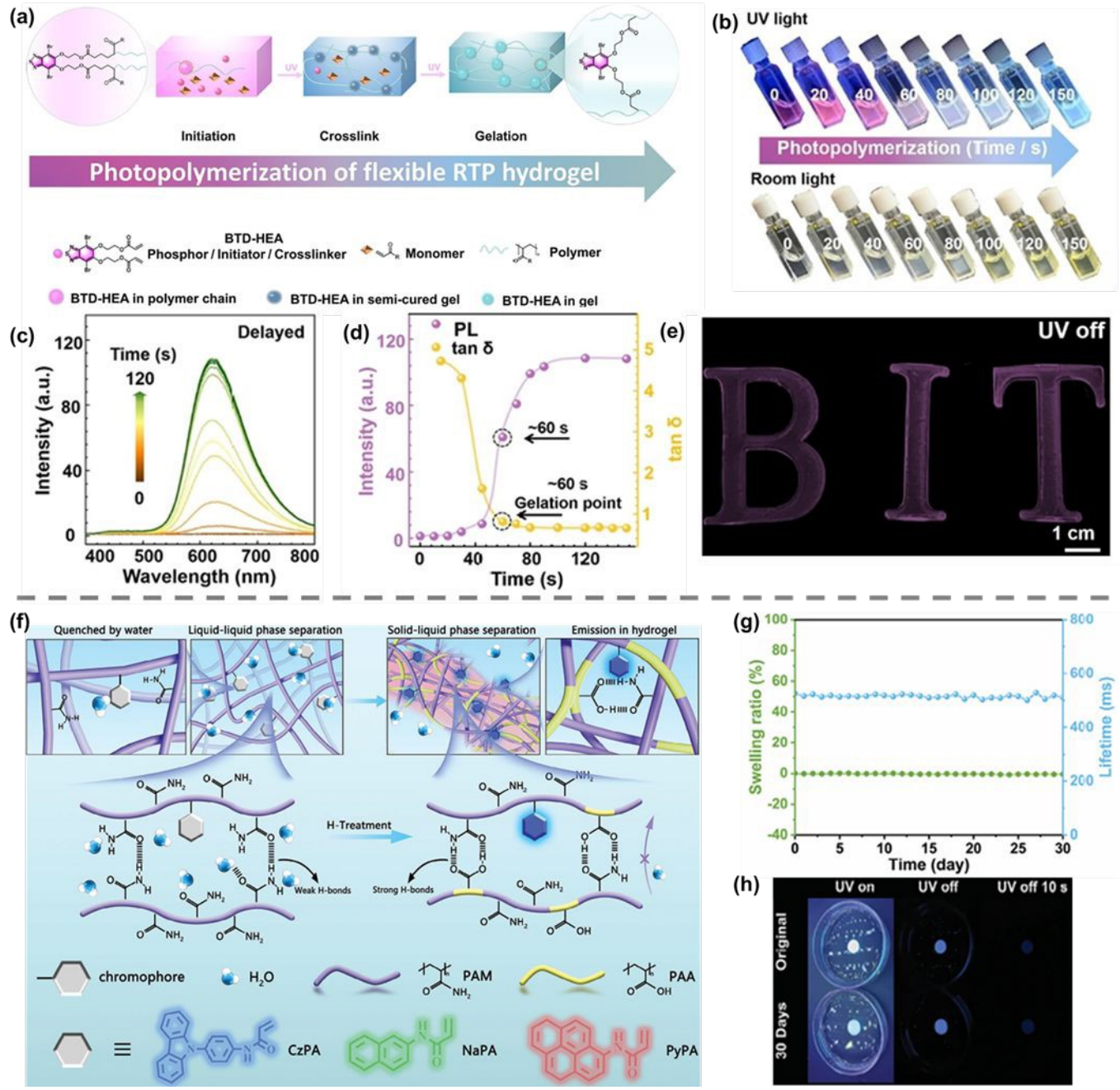

Fig. 7 Chemical grafting chromophores into polymeric RTP hydrogels. (a) The multifunctional phosphorescent compound of BTD-HEA initiates polymerization to generate gel. (b-c) Photos and delayed emission spectra intensity of BTD-HEA with AAm (3 wt%), captured at various stages during the gelation process under 365 nm UV light. (d) Delayed emission spectra intensity and loss factors of the gelation system with time. (e) Photos of the PHEA hydrogels phosphorescence emission after deactivating the UV-365 nm excitation source. (f) Mechanism of H-CzPA-co-PAM hydrogels induced by in-situ phase separation. This process prevents the non-radiative transition of the chromophore, allowing sustainable underwater emission. (g) Swelling ratio and phosphorescence lifetime of H-$CzPA_{0.10\%}$-co-PAM hydrogel with 9 h of H-treatment after placing in water for 30 days. (h) Afterglow photos of original H-$CzPA_{0.10\%}$-co-PAM hydrogel with 9 h of H-treatment in water and after immersing in water for 30 days.

phosphorescence compared to those with banded spherulites. Surprisingly, the hydrogels with banded spherulites exhibited circularly polarized luminescence (CPL) (Fig. 8e, g). This luminescence comes from the aggregation of clusters constrained by the crystal, while the twisted crystalline fibers give the achiral luminescent clusters CPL. In addition to crystallization-induced carbonyl groups clustering in polymers, the aggregation of carbonyl groups clustering can also be achieved through salt-induced aggregation. In 2024, Zhao *et al.* proposed a new strategy for constructing polymeric RTP hydrogels via salt-induced aggregation. AA and diethylenetriamine (DETA) were copolymerized to prepare a polymer network, which was then immersed in a sodium bromide solution.[58] The salt treatment promotes hydrophobic aggregation in the hydrogel network. The

View Article Online
DOI: 10.1039/D5SC00425G

resulting dense structure enabled the clustering of carboxyl groups and oxygen atoms, suppressing non-radiative transitions and thereby enabling RTP emission.

However, despite this impressive progress, the development of polymeric RTP hydrogels is still largely lagging, partially because of the tedious synthetic procedures. More efforts are thus suggested to exploring new and simple synthetic methods or the employment of well-organized supramolecular interactions in order to construct powerful polymeric RTP hydrogels.

3.3 Polymeric RTP hydrogels via supramolecular polymerization

Polymeric RTP hydrogels can also be constructed through the spontaneous self-assembly process of supramolecular polymerization of phosphorescence molecules and copolymer monomer molecules. The rigid microenvironment in hydrogels can be constructed through the process of supramolecular self-assembly, enabling RTP emission. Supramolecular polymerization is usually driven by electrostatic interactions, hydrogen bonds, dipole-dipole interactions, etc. Compared with physically doped polymeric hydrogels and chemically crosslinked polymeric hydrogel systems, supramolecular interactions exhibit high dynamism and reversibility, showing great application potential.

Electrostatic interactions are typical supramolecular interactions between ions with opposite charges (e.g., cations such as quaternary ammonium groups or protonated amino groups and anions such as carboxylate or sulfate groups). The supramolecular interaction sites are formed by the interaction between the chromophores and the group with opposite charge, and the polymeric RTP hydrogel can be prepared by supramolecular polymerization/crosslinking based on electrostatic interaction. For example, in 2021, Garain *et al.* synthesized a simple heavy atom-substituted cationic phthalimide derivative (CPthBr). After that, the researchers used the organic–inorganic supramolecular scaffolding strategy to form supramolecular action sites through the electrostatic interactions between CPthBr and the negatively charged laponite (LP) clays (Fig. 9a).[59] As LP was continuously added to the aqueous olution of CPthBr, the RTP emission peak about 487 nm was continuously enhanced (Fig. 9b). The phosphorescence lifetime was 1.62 ms (Fig. 9c). At higher LP concentrations, the LP scaffold

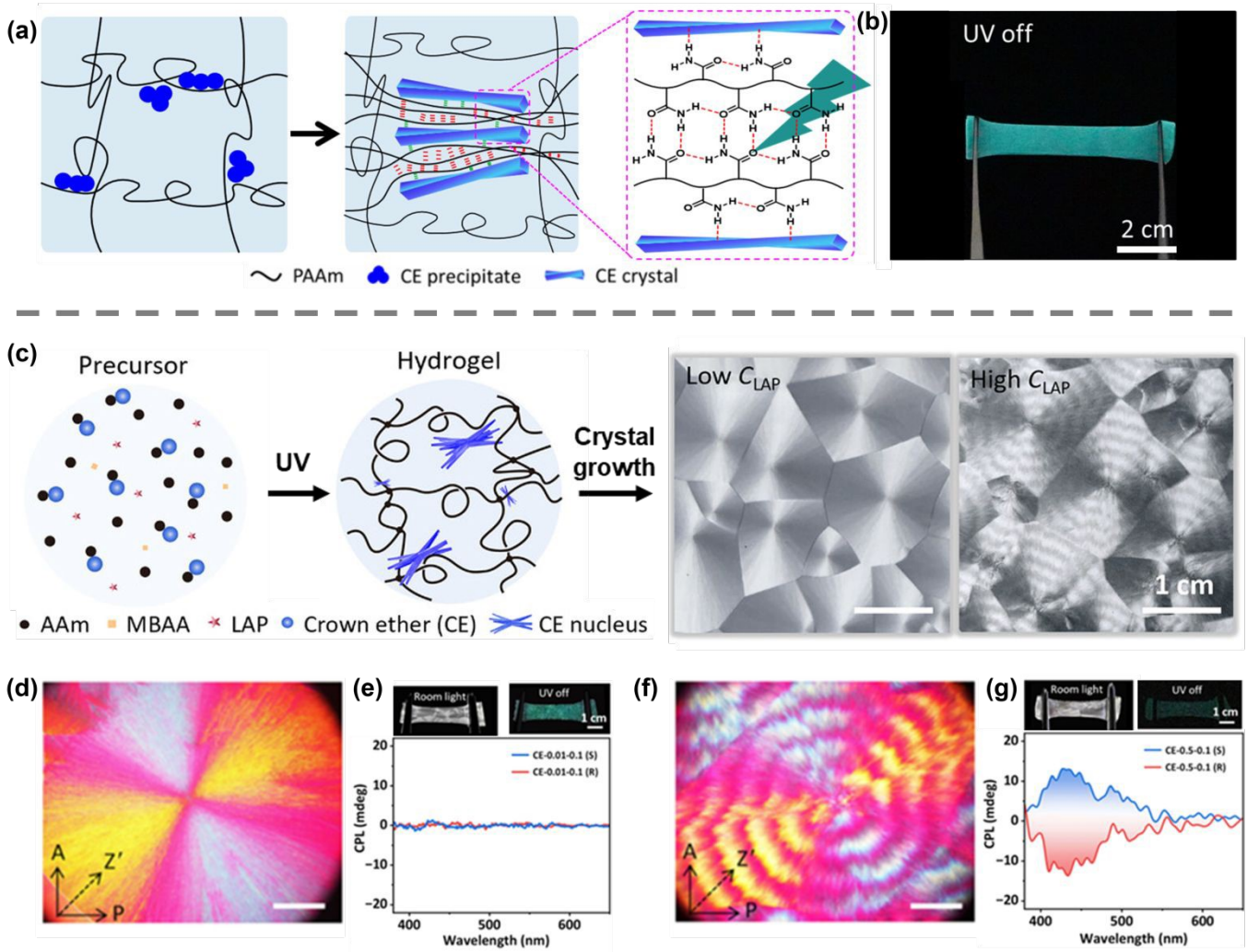

Fig. 8 Chemical grafting chromophores into polymeric RTP hydrogels. (a) Polymerization-induced crystallization of dopant molecules to form crystals that squeeze and confine the polymeric matrix as cluster phosphors of the composite hydrogel. (b) Photos of the CE-PAAm gel after being stretched to a strain of 100% after turning off 280 nm UV light. (c) Photopolymerization-induced crystallization of dopant molecules to form different spherulites in CE hydrogels and photos of composite hydrogels synthesized with low and high initiator LAP concentrations taken under room light, respectively. (d) Polarized optical micrographs of regular spherulites in CE-0.01-0.1 gel. (e) Photos showing the stretchability of CE-0.01-0.1 gels under room light and turning off the 280 nm UV light. Corresponding CPL spectra of gels with D/L-methionine excited at 280 nm are shown below. (f) Polarized optical micrographs of banded spherulites

in CE-0.5-0.1 gel. (g) Photos showing the stretchability of CE-0.5-0.1 gels under room light and turning off the 280 nm UV light. Corresponding CPL spectra of gels with D/L-methionine excited at 280 nm are shown below.

View Article Online
DOI: 10.1039/D5SC08423G

promoted the orderly arrangement of molecules through electrostatic interactions to form a unique self-standing supramolecular RTP hydrogels. Efficient triplet to singlet FÖrster resonance energy transfer process and delayed fluorescence were achieved by doping Sulforhodamine G (SRG) and Sulforhodamine101 (SR101) dyes into the CPthBr-LP hydrogels. Yellow and orange RTP hydrogels can be produced with average lifetimes of 162 μs and 55 μs, respectively (Fig. 9d).

Hydrogen bonds are also important supramolecular interactions for constructing supramolecular polymeric RTP hydrogels. Usually, a single hydrogen bond is too weak to stabilize supramolecular materials, but the synergistic effect of hydrogen bonds and other supramolecular interactions is conducive to the preparation of supramolecular polymeric hydrogels. For example, in 2024, Dai *et al.* developed the near-infrared (NIR) RTP supramolecular hydrogels based on amphiphilic bromonaphthalimide pyridinium derivative (G), LP nanosheets and PAAm. Initially, G molecules can self-assemble into positively charged spherical nanoparticles without RTP properties. Driven by electrostatic interactions, these nanoparticles can be co-assembled with negatively charged LP to form supramolecular RTP hydrogels (Fig. 9e).[60] This hydrogel exhibits red RTP phosphorescence at 586 nm with a lifetime of 4.03 ms. Furthermore, the physical crosslinking network is enhanced by introducing PAAm into the supramolecular RTP hydrogel system. The abundant hydrogen bonding intensifies RTP intensity and improves lifetime to 4.20 ms (Fig. 9f, g). In particular, the RTP emission can still be achieved at higher temperature (363K) with a lifetime of 2.46 ms (Fig. 9h, i).

Fig. 9

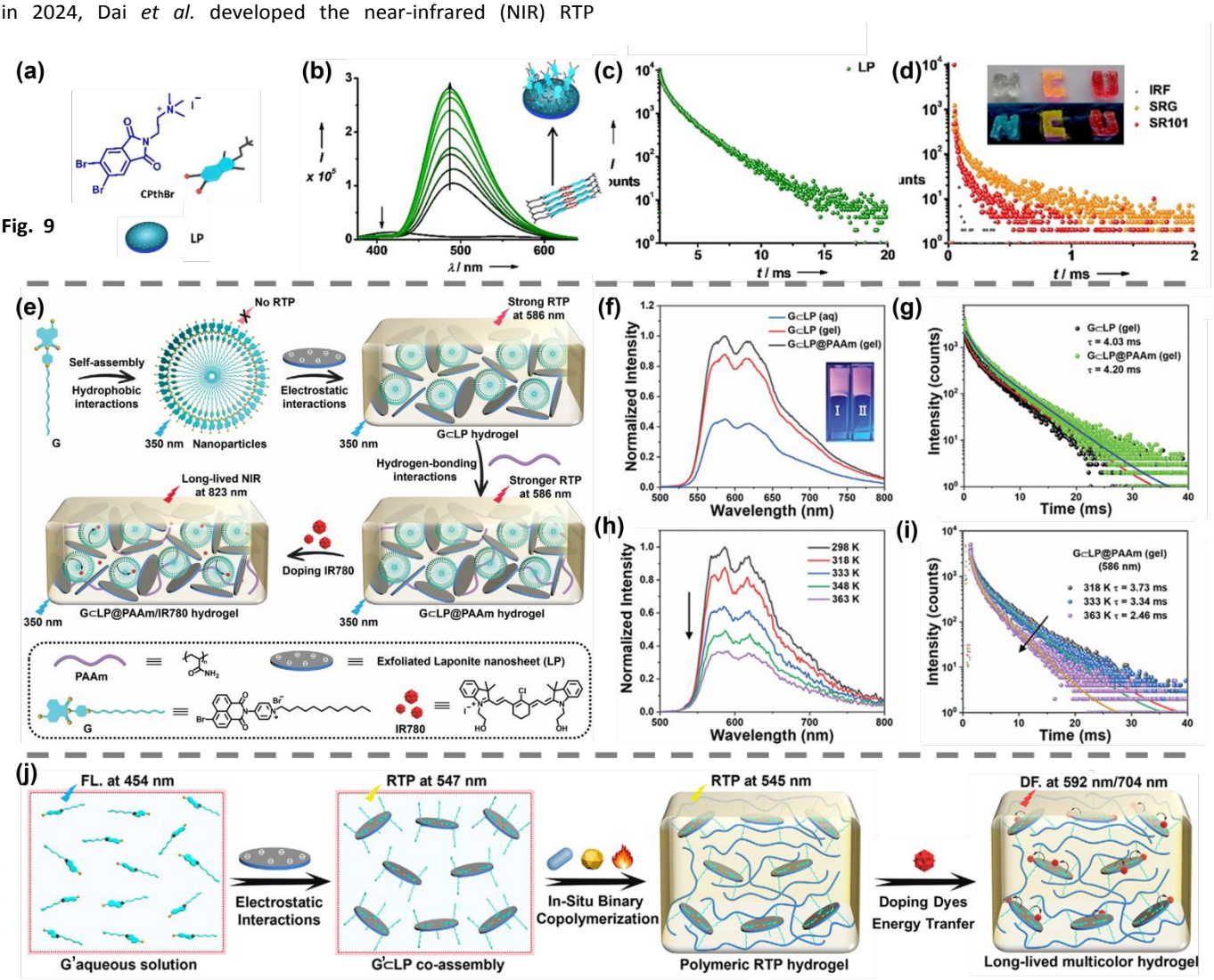

Polymeric RTP hydrogels via supramolecular polymerization. (a) Molecular structure and schematic representation of CPthBr and LP. (b) Photoluminescence titration study of the CPthBr with increasing the LP wt. % (0.125 wt% to 6 wt%) in an aqueous solution. (c) Lifetime decay plot of CPthBr-LP hybrid. (d) Delayed fluorescence lifetime decay plot of 10:1 CPthBrSRG-LP and CPthBr-SR101-LP hybrid hydrogels. Inset: Photos of self-standing hydrogel and "NCU" is written under visible light and under 254 nm UV light using hydrogel. (e) Schematic illustration of the preparation of NIR G⊂LP@PAAm hydrogels based on amphiphilic bromonaphthalimide pyridinium hierarchical assembly. (f) Phosphorescence emission spectra of G⊂LP (aq), G⊂LP hydrogel and G⊂LP@PAAm hydrogel. (g) Time-resolved photoluminescence decay spectra of G⊂LP hydrogel and G⊂LP@PAAm hydrogel at 410 nm. (h) Normalized phosphorescence emission spectra of G⊂LP@PAAm hydrogel at different temperatures. (i) Time-resolved photoluminescence decay spectra of G⊂LP@PAAm hydrogel at 318, 333, and 363 K. (j) Schematic representation of the construction of the robust G'⊂LP@PAAm hydrogels via green in situ copolymerization in aqueous solution.

View Article Online
DOI: 10.1039/D5SC08423G

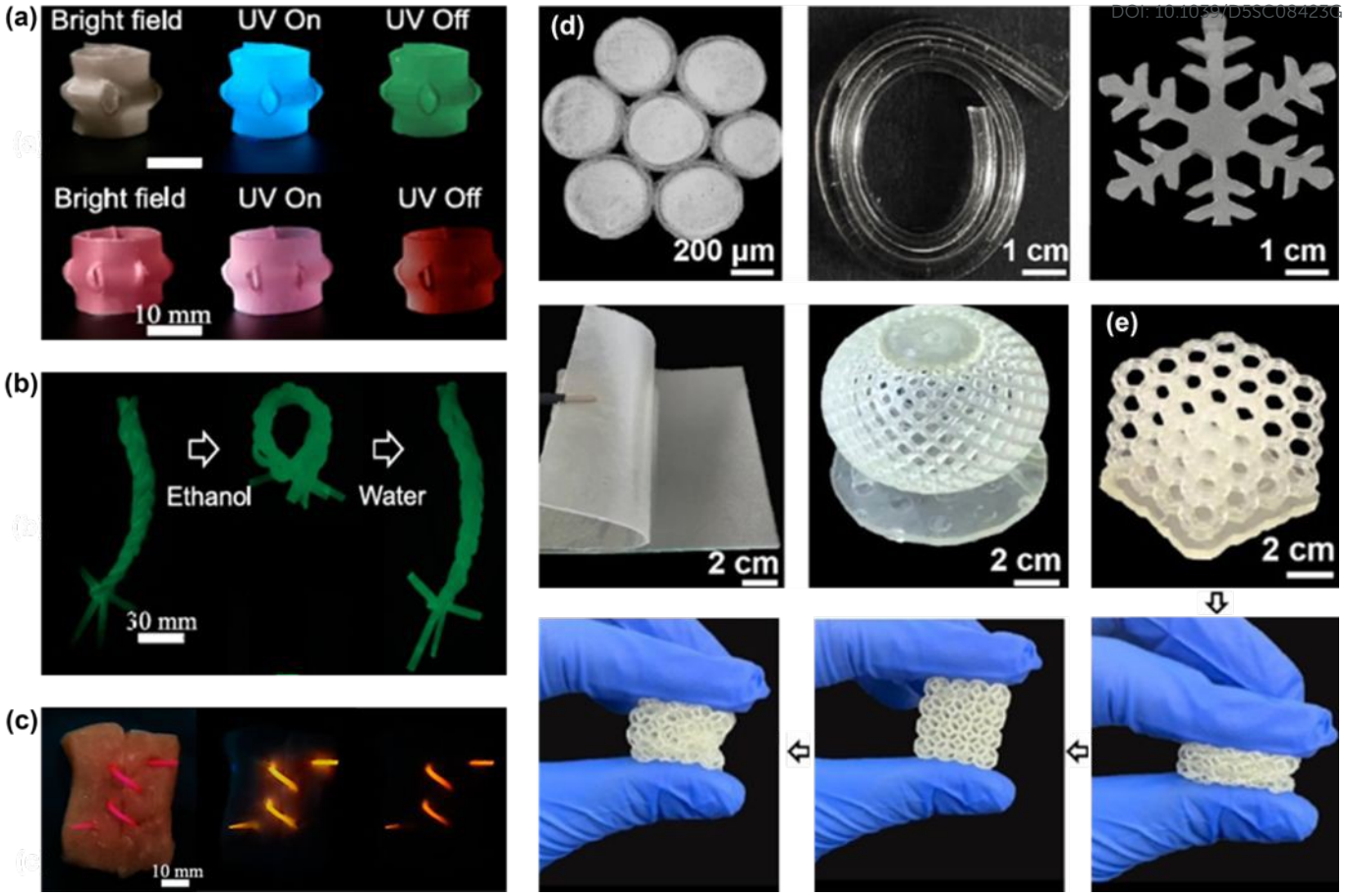

Fig. 10 Applications in 3D printing. (a) Afterglow images of 3D shapes from W-hydrogel and Rhodamine B-doped W-hydrogel. (b) RTP images of textiles made from W-hydrogel threads reversibly treated by ethanol and water. (c) Digital, fluorescent, and afterglow images of pork tissues sutured using RhB@W-hydrogel threads. (d) Photos illustrating the fibers, snowflake pattern, coating and 3D object prepared by the photo polymerization reaction with the BTD-HEA. (e) The lattice maintained its structural integrity after repeated compression.

Similarly, in 2025, they further prepared the supramolecular polymeric RTP hydrogels based on electrostatic interactions and hydrogen bonding synergy through green one-pot copolymerization of monoalkene-functionalized iodoisoquinolinium derivatives (G'), LP, and AAm monomers in aqueous solution (Fig. 9j).[61] This approach circumvents the multi-step assembly procedures employed in previous studies, thereby facilitating the construction of supramolecular polymeric RTP hydrogels.

Dipole-dipole interactions play an important role in supramolecular polymerization. By rationally designing the polar groups in the molecules, the molecules can be induced to self-assemble into nanoscale structural units, and then further polymerized into hydrogels. The formation of these supramolecular polymeric hydrogels typically relies not only on dipole-dipole interactions, but also on other types of supramolecular interactions. For example, in 2023, Xin *et al.* designed supramolecular polymeric RTP hydrogels prepared by simply heating/mixing and cooling hexamethyl cucurbit[5]uril (HmeQ[5]) and 1,4-diaminobenzene (DB).[62] HmeQ[5] has two ports surrounded by carbonyl groups. The dipole-dipole interaction and hydrogen bonding between it and the amino group of protonated DB played an important role in the supramolecular polymerization process. Scanning Electron Microscope (SEM) showed the morphology of the freeze-dried hydrogel, exhibiting a fiber network structure. The incorporation of chromophores induces stimulated RTP emission in the ordered fiber structure of the supramolecular hydrogel, effectively suppressing non-radiative transitions. This effect can be proved by the imaging study of laser confocal microscope. Meanwhile, due to the temperature sensitivity of the supramolecular interactions, a sol-to-gel transition was observed when the hydrogels were cooled to 25 °C, while a gel-to-sol transition was observed in the temperature of 75 °C.

4. Applications of polymeric RTP hydrogels

Polymeric RTP hydrogels, as a new generation of intelligent materials hold immense application potential due to their outstanding biocompatibility, flexible and stretchable mechanical properties, as well as three-dimensional porous network structure.[63-68] In terms of optical performance, its unique long-term stability, tunability, and stimulus-responsive luminescence characteristics make it highly promising for applications in 3D printing, bioimaging, and complex information encryption technologies. This section will briefly summarize the application progress of RTP hydrogels in these fields.

View Article Online
DOI: 10.1039/D5SC08423G

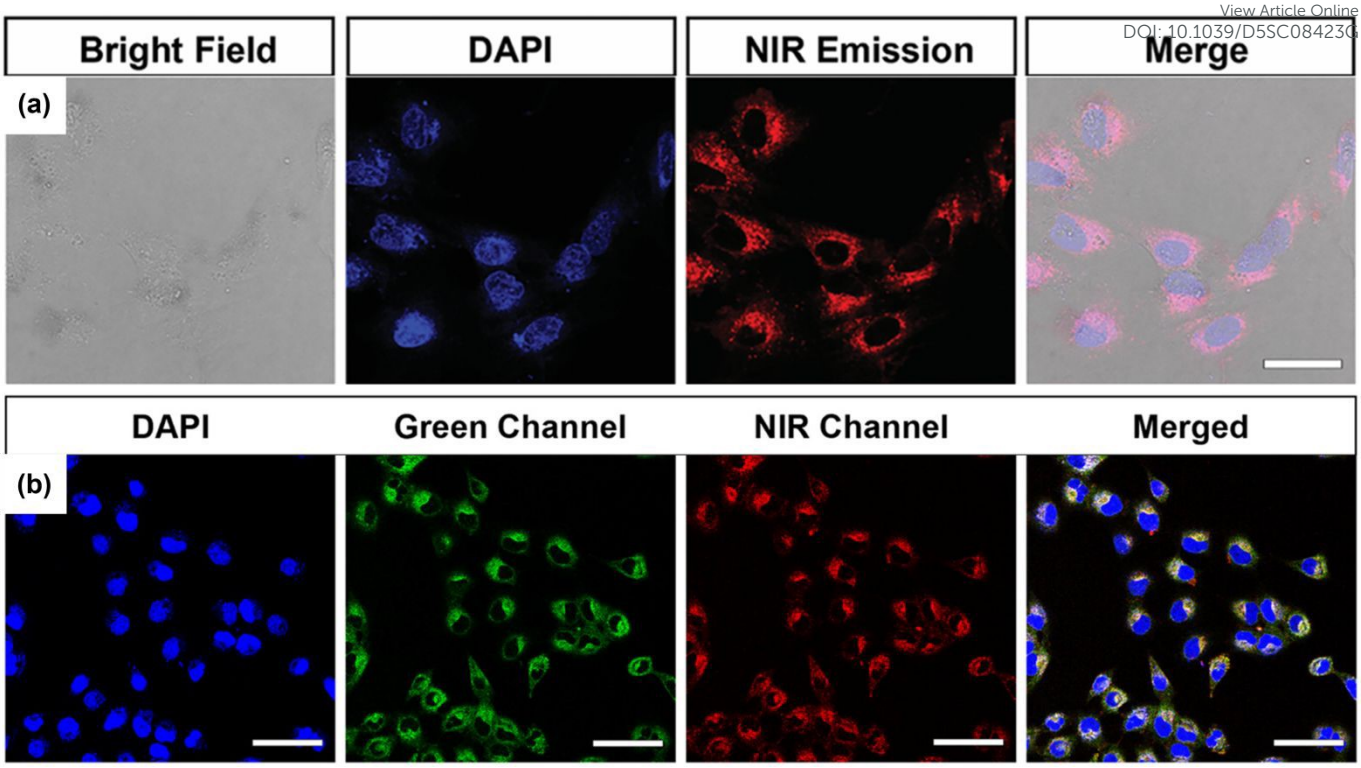

Fig. 11 Applications in bioimaging. (a) Cellular imaging of living HeLa cancer cells stained by G⊂LP@PAAm/IR780. The nuclei stained by 4,6-diamidino-2phenylindole (DAPI, blue) was collected from 420 to 470 nm, while the NIR emission was observed from 700 to 800 nm, respectively (Scale bar = 25 μm). (b) G⊂LP@PAAm/Rh800. The nuclei stained by 4,6diamidino-2-phenylindole (DAPI, blue) were acquired from 420 to 470 nm (Scale bar = 60 μm).

4.1 3D printing

Polymeric RTP hydrogels have the advantages of long lifetime, non-interference background and easy preparation into 3D shapes.[69-70] In previous work, polymeric RTP hydrogels were processed into 3D shapes with distinct luminescence (Fig. 10a).[51] Subsequently, these hydrogels were fabricated into micron-sized hydrogel threads and applied to the suture of biological tissues (Fig. 10b, c). However, the hydrogels prepared using the template method exhibit low precision, making it challenging to fabricate polymeric RTP hydrogels with complex 3D macroscopic structures (such as porous scaffolds). 3D printing technology offers advantages in forming complex structures and achieving high precision. The photo-initiated polymerization and rheological properties enable the 3D printing of polymeric RTP hydrogels (Fig. 10d).[46] This fabrication process achieved micron-scale precision and produced structures with outstanding mechanical performance. Importantly, the printed lattice structures maintained their completeness even after multiple repeated compression cycles (Fig. 10e).

4.2 Bioimaging

In the field of bioimaging, the core challenge restricting the sensitivity and accuracy of imaging is how to accurately extract the target signal from the complex and auto-fluorescence biological background.[71-75] With advancing research, certain polymeric RTP hydrogels have ultra-long emission lifetimes of milliseconds or even seconds. Researchers can use time-resolveimaging technology to collect long-lived RTP signals after the complete decay of short-lived background fluorescence, thereby achieving ultra-high signal-to-noise ratio imaging. For example, a NIR RTP supramolecular hydrogels was developed based on amphiphilic bromonaphthalimide pyridinium derivatives, nanosheets (LP), AAm and heptamethine cyanine. The hydrogel exhibits low cytotoxicity and good biocompatibility. The NIR emission signal of the RTP hydrogel in HeLa cells was observed by laser scanning microscopy, revealing distinct cellular contours (Fig. 11a).[60] In addition, a NIR RTP hydrogels constructed through supramolecular polymerization using monoalkene-functionalized iodoisoquinolinium derivatives (G'), LP, rhodamine 800 ((Rh800)) and AAm monomers can also achieve similar effects (Fig. 11b). [61]

4.3 Anti-counterfeiting encryption

In addition, the tunable luminescent performance and stimulus responsiveness of polymeric RTP hydrogels provide significant application value in the field of information anti-counterfeiting encryption.[76-79]

Wu's group used the quenching effect of halogen ions on polymeric RTP hydrogels and the fluorescein solution to make hydrogels display different information when the UV lamp was on and off, achieving information encryption. The strategy involves printing the real information "OFF" onto the hydrogel with KI solution. Then, the word "OPEN" is printed onto the hydrogel with fluorescein solution to cover and encrypt the word "OFF". When irradiated under UV lamp, the area printed with fluorescein showed bright yellow fluorescence, showing the word "OPEN". Upon removal of the UV lamp, the KI printed area reveals the true information "OFF" due to the difference in phosphorescence intensity between the quenched and unquenched area (Fig. 12a).[56]

The polymeric RTP hydrogels with excitation wavelength-dependent luminescence provide more possibilities for

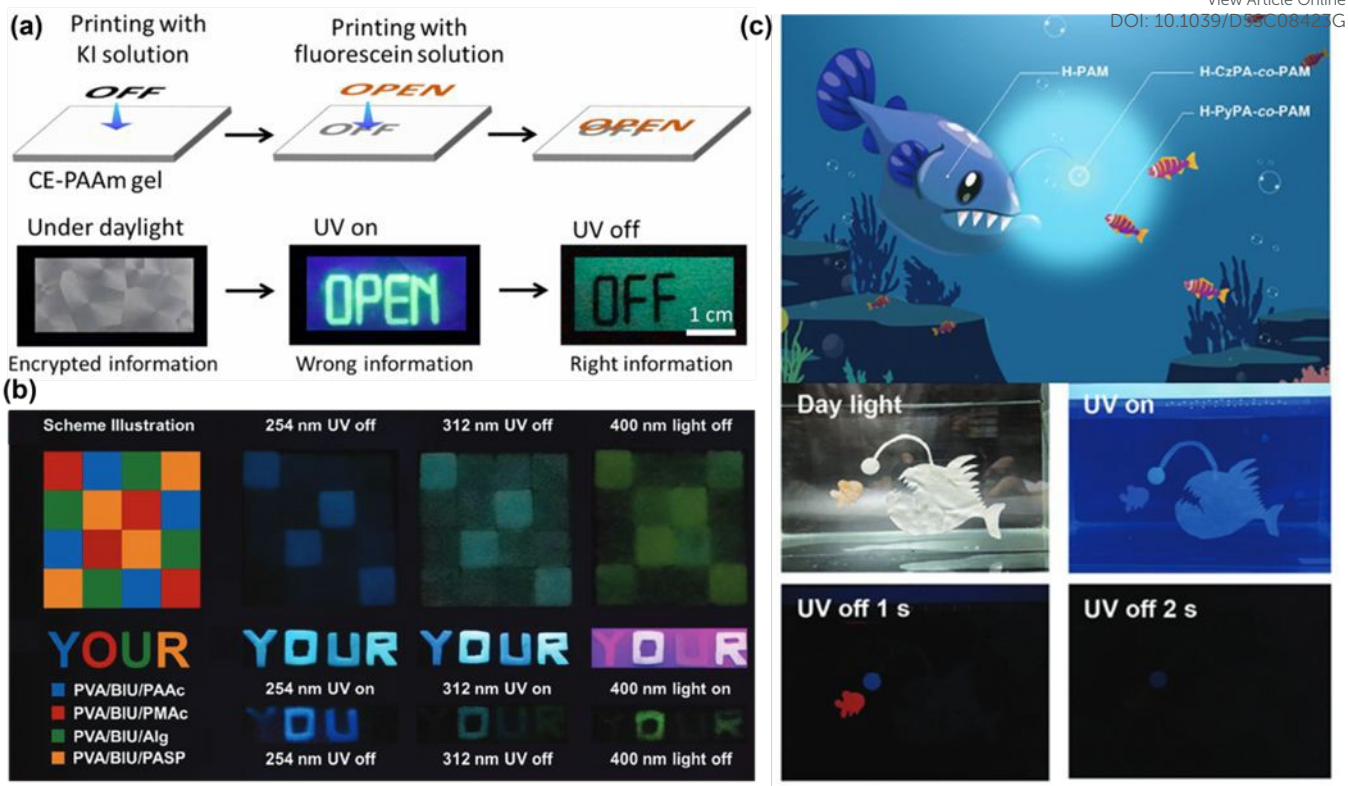

Fig. 12 Applications in anti-counterfeiting encryption (a) Schematic and photos for the encoding of digital information by printing of KI solution and fluorescein solution on the CE-PAAm gel. (b) Schematic illustration and photos of patterns composed of different hydrogels (PVA/BIU/acid, acid = PASP, PAAc, Alg, PITAc, and PMVPAc) showing different information after excited under different wavelengths irradiation. (c) Demonstration of camouflage of marine animals.

information encryption. Wang's group obtained a series of excitation wavelength-dependent RTP hydrogels by changing the acid component in the hydrogel (PVA/BIU/PMAc) to alginic acid (Alg), poly(itaconic acid) (PITAc) and poly(maleic acid-co-vinyl pyrrolidone) (PMVPAc). The information code was constructed by hydrogel squares with different compositions，which can display various patterns under different wavelengths of excitation. Additionally, several types of hydrogels were used to form the letters "Y," "O," "U," and "R.", respectively. Under the excitation of 254, 312 and 400 nm light, all patterns show the word "YOUR". However, after turning off the light sources at these respective wavelengths, the patterns of "YOU", "OUR" and "OR" can be observed separately (Fig. 12b).[50]

Furthermore, the Lü's group replaced the grafted chromophores in the polymeric RTP hydrogel (H-CzPA-co-PAM) with N-1-pyrenyl-2-propenamide (PyPA) to achieve the regulation of the afterglow color and duration. And a conceptual camouflage skin of marine animals was proposed. As shown in Fig. 12C, different polymeric RTP hydrogels were used as multiple functional skins of different deep-sea fishes. After removing the 365 nm UV excitation, the blue lure of the anglerfish will attract other fish (such as the eyelight fish, which is marked in red) due to the phototaxis of most deep-sea fish preying. The blue lure can also be used for communication between the same species. After removing the 365 nm UV excitation for 2 s, the blue lure was intelligently observed due to the difference in the afterglow time of different polymeric RTP hydrogels, achieveing the underwater dynamic temporal information display. [55]

5. Summary and Outlook

In summary, polymeric RTP hydrogels are highly sensitive to environmental conditions, particularly water and oxygen, which lead to rapid quenching.. The solution to these challenges lies in providing a rigid microenvironment for chromophores in the hydrogels to inhibit non-radiative transitions, thereby achieving RTP emission.This review systematically summarized the construction strategies for polymeric RTP hydrogels, including: physical doping, chemical grafting, and supramolecular polymerization. Furthermore, the applications of RTP hydrogels in 3D printing, bioimaging, and anti-counterfeiting technology are outlined. Undoubtedly, RTP hydrogels have made significant progress in achieving multifunctionality and stable afterglow, primarily through innovative molecular design and structural design of polymeric hydrogel networks. However, several critical shortcomings remain to be addressed: 1. The luminous efficiency is lower than that of traditional rigid RTP materials, and the RTP lifetime is relatively short. 2. There are still difficulties in the transition from small-scale laboratory preparation to industrial production. 3. The RTP performance varies at different positions during the 3D printing process 4. Design multi-stimuli responsive polymeric RTP hydrogels. 5. UV excitation is commonly required to achieve RTP emission. 6. Achieving full-spectrum RTP luminescence remains challenging, especially NIR phosphorescence.

Given these challenges, future research should focus more on the following areas: First, it is necessary to improve the performance of polymeric RTP hydrogels by developing new chromophores and innovative polymer structure designs. Thus, on the premise of ensuring the advantages of hydrogels flexibility, efforts should aim to endow polymeric RTP hydrogels with higher luminous efficiency, longer RTP lifetime, and wider spectral

emission range. The advancement of high-performance RTP hydrogels will drive technological innovations in fields such as information anti-counterfeiting.

Secondly, the synthetic routes of efficient organic RTP molecules are usually complex, involving multiple reaction steps, with relatively low yields. While gram-scale preparation is feasible, challenges arise when scaling up to kilogram- or ton-scale production. The key indicators such as the RTP properties of the final product may fluctuate between batches, making it difficult to meet the stringent stability requirements for industrial products. The same problem also occurs in the 3D printing process, due to the stability of the prepared RTP polymer ink and the layer-by-layer accumulation process of 3D printing. This leads to inconsistent RTP properties in different positions of 3D printed products, as well as poor stability between batches. Whether it is large-scale production or 3D printing, the future breakthrough direction lies in the deep integration of molecular design, material engineering and process innovation.

In addition, the hydrogels network can respond to external stimuli (such as pH, temperature, and specific molecules), resulting in changes in volume or conformation, and then manipulating the RTP emission, providing new opportunities for the design of multi-stimulus response polymeric RTP hydrogels. The advantage of multi-stimulus response polymeric RTP hydrogels is that they break the linear mode of "single stimulus-single response", and then turn to the networked mode of "multi-input-intelligent processing-multi-dimensional output". Thus, intelligent materials that can sense complex environments and make readable responses are constructed. This provides a new strategy for applications in advanced sensing, information anti-counterfeiting, and other fields.

Finally, most traditional RTP materials require high-energy ultraviolet light excitation, which possesses strong penetration and energy, potentially causing various damages to biological tissues. In contrast, visible light-excited RTP does not need to worry about the above problems, offering vast application in cutting-edge fields such as bioimaging and intelligent sensing. Owing to the deeper tissue penetration and lower biological background interference of NIR phosphorescence, the development of efficient NIR RTP hydrogels will be a key step in achieving deep, high-resolution in vivo imaging, which is extremely challenging and valuable. In addition, there have been relatively few biocompatibility tests conducted on the application of polymeric RTP hydrogels in the field of bioimaging. Related studies for bioimaging should conduct a comprehensive assessment of biocompatibility, including cytotoxicity and blood compatibility, to ensure that the imaging process does not cause damage to the organism. In addition, the biodistribution and metabolic pathways of polymeric RTP hydrogels should be studied by in vivo imaging system, and the systemic distribution, organ enrichment and clearance time of polymeric RTP hydrogels (or their degradation products) after injection or implantation should be dynamically monitored to assess their safety in bioimaging applications.

In conclusion, research on polymeric RTP hydrogels has moved from basic material synthesis to the development of function-oriented intelligent devices. It provides innovative solutions to solve the challenging problems in the fields of biomedicine and information technology.

Author contributions

Tao Chen supervised the manuscript. Wei Lu and Xiaoye Zhang revised the manuscript. Weihao Feng. wrote the manuscript. Muqing Si and Kuangzheng Cao were contributed to the manuscript preparation. All authors revised and finalized the manuscript.

Conflicts of interest

View Article Online
DOI: 10.1039/D5SC08423G

The authors declare no conflicts of interest.

Data availability

No primary research results, sofware or code have been included and no new data were generated or analyzed as part of this review.

Acknowledgements

This work was supported by Zhejiang Provincial Natural Science Foundation of China under Grant No. LR23E030001.

References

1 Z. Li, X. Ji, H. Xie, B. Z. Tang, *Adv. Mater.* 2021, **33**, 2100021.
2 S. Cai, Z. Sun, H. Wang, X. Yao, H. Ma, W. Jia, S. Wang, Z. Li, H. Shi, Z. An, Y. Ishida, T. Aida, W. Huang, *J. Am. Chem. Soc.* 2021, **143**, 16256–16263.
3 X. Ma, J. Wang, H. Tian, *Acc. Chem. Res.* 2019, **52**, 738–748.
4 J. Guo, C. Yang, Y. Zhao, *Acc. Chem. Res.* 2022, **55**, 1160–1170.
5 L. Li, J. Zhou, J. Han, D. Liu, M. Qi, J. Xu, G. Yin, T. Chen, *Nat. Commun.* 2024, **15**, 3846.
6 H. Sun, Q. Zhang, L. Meng, Z. Wang, Y. Fan, M. Mayor, M. Pan, C.-Y. Su, *Chem. Sci.* 2024, **15**, 8905–8912.
7 H. Shi, W. Yao, W. Ye, H. Ma, W. Huang, Z. An, *Acc. Chem. Res.* 2022, **55**, 3445-3459.
8 K. Benson, A. Ghimire, A. Pattammattel, C. V. Kumar, *Adv. Funct. Mater.* 2017, **27**, 1702955.
9 X. Yu, A. A. Ryadun, D. I. Pavlov, T. Y. Guselnikova, A. S. Potapov, V. P. Fedin, *Adv. Mater.* 2024, **36**, 2311939.
10 Z. Zhang, L. Qian, B. Zhang, C. Ma, G. Zhang, *Angew. Chem. Int. Ed.* 2024, **63**, e202410335.
11 Q. Dang, Y. Jiang, J. Wang, J. Wang, Q. Zhang, M. Zhang, S. Luo, Y. Xie, K. Pu, Q. Li, Z. Li, *Adv. Mater.* 2020, **32**, 2006752.
12 Y. Fan, S. Liu, M. Wu, L. Xiao, Y. Fan, M. Han, K. Chang, Y. Zhang, X. Zhen, Q. Li, Z. Li, *Adv. Mater.* 2022, **34**, 2201280.
13 M. Cui, P. Dai, J. Ding, M. Li, R. Sun, X. Jiang, M. Wu, X. Pang, M. Liu, Q. Zhao, B. Song, Y. He, *Angew. Chem. Int. Ed.* 2022, **61**, e202200172.
14 F. Xiao, H. Gao, Y. Lei, W. Dai, M. Liu, X. Zheng, Z. Cai, X. Huang, H. Wu, D. Ding, *Nat. Commun.* 2022, **13**, 186.
15 M. Yao, W. Wei, W. Qiao, Y. Zhang, X. Zhou, Z. Li, H. Peng, X. Xie, *Adv. Mater.* 2025, 2414894.
16 H. Yang, S. Li, J. Zheng, G. Chen, W. Wang, Y. Miao, N. Zhu, Y. Cong, J. Fu, *Adv. Mater.* 2023, **35**, 2301300.
17 H. Zhang, B. Zhang, C. Cai, K. Zhang, Y. Wang, Y. Wang, Y. Yang, Y. Wu, X. Ba, R. Hoogenboom, *Nat. Commun.* 2024, **15**, 2055
18 W. Luo, L. Chen, G. Yin, C. Yue, S. Xie, J. Zhou, W. Feng, Y. Nie, H. Qiu, F. Li, S. Cai, Y. Li, Z. Cai, T. Chen, *Angew. Chem. Int. Ed.* 2025, **64**, e202423650.
19 Kenry; C. Chen; B. Liu, *Nat. Commun.* 2019, **10**, 2111.
20 C. Chen, Z. Chi, K. Chong, A.S. Batsanov, Z. Yang, Z. Mao, Z. Yang, B. Liu, *Nat. Mater.* 2021, **20**, 175−180.
21 X.-Y. Dai, M. Huo, Y. Liu, *Nat. Rev. Chem.* 2023, **7**, 854–874.
22 D. Li, Z. Liu, M. Fang, J. Yang, B. Z. Tang, Z. Li, *ACS Nano* 2023, **17**, 12895–12902.
23 M. Roucan, M. Kielmann, S. J. Connon, S. S. R. Bernhard, M. O. Senge, *Chem. Commun.* 2018, **54**, 26–29.
24 Q. Yu, Z. Deng, R. Chen, J. Zhang, R. T. K. Kwok, J. W. Y. Lam, J. Sun, B. Z. Tang, *J. Am. Chem. Soc.* 2025, **147**, 10530–10539.

25 S. Garain, S. N. Ansari, A. A. Kongasseri, B. Chandra Garain, S. K. Pati, S. J. George, *Chem. Sci.* 2022, **13**, 10011.
26 Y. Deng, P. Chen, X. Yang, N. Li, S. Ma, Z. Huang, S. Lü, *Adv. Mater.* 2025,37 e14693.
27 F. Nie, D. Yan, *Angew. Chem. Int. Ed.* 2023, **62**, e202302751.
28 B. Zhou, Z. Qi, D. Yan, *Angew. Chem. Int. Ed.* 2022, **61**, e202208735.
29 Y. N. Ye, K. Cui, W. Hong, X. Li, C. Yu, D. Hourdet, T. Nakajima, T. Kurokawa, J. P. Gong, *Proc. Natl. Acad. Sci. U.S.A.* 2021, **118**, e2014694118.
30 W. Lu, M. Si, X. Le, T. Chen, *Acc. Chem. Res.* 2022, **55**, 2291–2303.
31 M. Hua, S. Wu, Y. Ma, Y. Zhao, Z. Chen, I. Frenkel, J. Strzalka, H. Zhou, X. Zhu, X. He, *Nature* 2021, **590**, 594–599.
32 L. Chen, Z. Jin, W. Feng, L. Sun, H. Xu, C. Wang, *Science* 2024, **383**, 1455–1461.
33 G. Zhang, J. Steck, J. Kim, C. H. Ahn, Z. Suo, *Sci. Adv.* 2023, **9**, eadh7742.
34 W. Li, X. Wang, Z. Liu, X. Zou, Z. Shen, D. Liu, L. Li, Y. Guo, F. Yan, *Nat. Mater.* 2024, **23**, 131–138.
35 X. Yao, J. Wang, D. Jiao, Z. Huang, O. Mhirsi, F. Lossada, L. Chen, B. Haehnle, A. J. C. Kuehne, X. Ma, H. Tian, A. Walther, *Adv. Mater.* 2021, **33**, 2005973.
36 C. Zheng, S. Tao, X. Zhao, C. Kang, B. Yang, *Angew. Chem. Int. Ed.* 2024, **63**, e202408516.
37 J. Xiao, J. Deng, X. Wang, H. Ho, C. Bai, Y. Bai, H. Wang, *Small* 2024, **20**, 2405615.
38 Y. Zhang, Y. Su, H. Wu, Z. Wang, C. Wang, Y. Zheng, X. Zheng, L. Gao, Q. Zhou, Y. Yang, X. Chen, C. Yang, Y. Zhao, *J. Am. Chem. Soc.* 2021, **143**, 13675–13685.
39 S. Tang, S. Jiang, K. Wang, Y. Zhang, L. Yi, J. Hou, L. Qu, Y. Zhao, C. Yang, *Adv. Mater.* 2025, **37**, 2416397.
40 Z. Man, Z. Lv, Z. Xu, J. He, Q. Liao, Y. Yang, J. Yao, H. Fu, *J. Am. Chem. Soc.* 2023, **145**, 13392–13399.
41 J. Li, L. Zhang, C. Wu, Z. Huang, S. Li, H. Zhang, Q. Yang, Z. Mao, S. Luo, C. Liu, G. Shi, B. Xu, *Angew. Chem. Int. Ed.* 2023, **62**, e202217284.
42 T. Zhu, S. Zheng, T. Yang, W. Z. Yuan, *J. Phys. Chem. Lett.* 2023, **14**, 6451–6458.
43 M. Qi, J. Huang, J. Wei, J. Zhou, D. Liu, L. Li, W. Luo, G. Yin, T. Chen, *Angew. Chem. Int. Ed.* 2025, **64**, e202501054.
44 X. Huang, Y. Zhang, G. Li, T. Wang, P. Sun, J. Shi, B. Tong, J. Zhi, Z. Li, Z. Cai, Y. Dong, *ChemPhotoChem* 2024, **9**, e202400315.
45 M. Fang, J. Yang, Z. Li, *Prog. Mater Sci.* 2022, **125**, 100914.
46 Y. Cao, D. Wang, Y. Zhang, G. Li, C. Gao, W. Li, X. Chen, X. Chen, P. Sun, Y. Dong, Z. Cai, Z. He, *Angew. Chem. Int. Ed.* 2024, 63, e202401331.
47 J. Deng, H. Liu, D. Liu, L. Yu, Y. Bai, W. Xie, T. Li, C. Wang, Y. Lian, H. Wang, *Adv. Funct. Mater.* 2024, **34**, 2308420.
48 X. Jiang, M. Wu, L. Zhang, J. Wang, M. Cui, J. Wang, X. Pang, B. Song, Y. He, *Anal. Chem.* 2022, **94**, 7264–7271.
49 Y. Sun, L. Jiang, Y. Chen, Y. Liu, *Chin. Chem. Lett.* 2024, **35**, 108644.
50 J. Deng, D. Liu, H. Liu, L. Yu, Y. Bai, J. Xiao, H. Wang, *Adv. Funct. Mater.* 2024, **34**, 2408821.
51 R. Liu, H. Guo, S. Liu, J. Li, S. Li, T. D. James, Z. Chen, *Nat. Commun.* 2024, **15**, 10588.
52 W. Feng, F. Li, Z. Jiang, C. Yue, G. Yin, N. Zhu, K. Zhang, T. Chen, W. Lu, *Angew. Chem. Int. Ed.* 2025, **64**, e202505192.
53 H. Chen, X. Ma, S. Wu, H. Tian, *Angew. Chem. Int. Ed.* 2014, **53**, 14149-14152.
54 H. Chen, L. Xu, X. Ma, H. Tian, *Polym. Chem*. 2016, **7**, 3989–3992.
55 P. Chen, H. Qie, X. Yang, S. Ma, Z. Wang, N. Li, Y. Deng, F. Bian, S. Lü, *Adv. Funct. Mater.* 2025, **35**, 2416430.
56 H. Ju, H. Zhang, L. X. Hou, M. Zuo, M. Du, F. Huang, Q. Zheng, Z. L. Wu, *J. Am. Chem. Soc.* 2023, **145**, 3763–3773.
57 Z. Zhang, H. Ju, H. Zhang, Z. Wang, M. Du, H. Li, F. Huang, Q. Zheng, Z. L. Wu, *Adv. Mater.* 2025, **37**, 2505444.
58 S. Yu, J. Zhang, X. Chen, X. Wu, X. Zhao, Z. Zhu, J. Zhang, Y. Zuo, C. Zhao, *Adv. Opt. Mater.* 2024, **12**, 2303330.
59 S. Garain, B. C. Garain, M. Eswaramoorthy, S. K. Pati, S. J. George, *Angew. Chem. Int. Ed.* 2021, **60**, 19720-19724.
60 Q. Song, Z. Liu, J. Li, Y. Sun, Y. Ge, X. Dai, *Adv. Mater.* 2024, **36**, 2409983.
61 Q. Song, Z. Liu, X. Bai, Y. Zhang, S. Yang, Y. Ge, X. Dai, *Adv. Opt. Mater.* 2025, **13**, 2500624.
62 X. Sun, H. Yang, W. Zhang, S. Zhang, J. Hu, M. Liu, X. Zeng, Q. Li, C. Redshaw, Z. Tao, X. Xiao, *ACS Appl. Mater. Interfaces* 2023, **15**, 4668–4676.
63 W. Zhao, Z. He, B. Z. Tang, *Nat. Rev. Mater.* 2020, **5**, 869–885.
64 G. Baryshnikov, B. Minaev, H. Ågren, *Chem. Rev.* 2017, **117**, 6500–6537.
65 H. Sun, M. He, G. V. Baryshnikov, B. Wu, R. R. Valiev, S. Shen, M. Zhang, X. Xu, Z. Li, G. Liu, H. Ågren, L. Zhu, *Angew. Chem. Int. Ed.* 2024, **63**, e202318159.
66 G. Yin, W. Lu, J. Huang, R. Li, D. Liu, L. Li, R. Zhou, G. Huo, T. Chen, *Aggregate* 2023, **4**, e344.
67 Z. Xie, P. Sun, Z. Wang, H. Li, L. Yu, D. Sun, M. Chen, Y. Bi, X. Xin, J. Hao, *Angew. Chem. Int.* Ed. 2020, **59**, 9922–9927.
68 J. Chen, F. Lin, D. Guo, T. Tang, Y. Miao, Y. Wu, W. Zhai, H. Huang, Z. Chi, Y. Chen, Z. Yang, *Adv. Mater.* 2024, **36**, 2409642.
69 H. Sun, Y. Xiao, Y. He, X. Wei, J. Zou, Y. Luo, Y. Wu, J. Zhao, V. K.-M. Au, T. Yu, *Chem. Sci.* 2025, **16**, 5299–5309.
70 P. Wu, P. Li, M. Chen, J. Rao, G. Chen, J. Bian, B. Lue, F. Peng, *Adv. Mater.* 2024, **36**, 2402666.
71 J. Zhu, L. Luo, M. Gu, Y. Chen, L. Wang, M. Li, X. Chen, X. Peng, *CCS Chem* 2025, **7**, 1552–1566.
72 J. Yuan, H. Yang, W. Huang, S. Liu, H. Zhang, X. Zhang, X. Peng, *Chem. Soc. Rev.* 2025, **54**, 341–366.
73 T. Xiong, Y. Chen, Q. Peng, M. Li, S. Lu, X. Chen, J. Fan, L. Wang, X. Peng, *J. Am. Chem. Soc.* 2024, **146**, 24158–24166.
74 H. Gao, T. Zhang, Y. Lei, D. Jiao, B. Yu, W. Z. Yuan, J. Ji, Q. Jin, D. Ding, *Angew. Chem. Int.* Ed. 2024, **63**, e202406651.
75 L. Li, D. Liu, J. Zhou, M. Qi, G. Yin, T. Chen, *Mater. Horiz.* 2024, **11**, 5895–5913.
76 Y. Shen, X. Le, Y. Wu, T. Chen, *Chem. Soc. Rev.* 2024, **53**, 606-623.
77 J. Xiang, Y. Shi, J. Jiang, J. Yan, S. Xiao, H. Lin, T. Yi, *Adv. Opt. Mater.* 2024, **12**, 2302671.
78 J. Wei, Y. Xiao, J. Luo, Z. He, J. Chen, Q. Peng, D. Kuang, *Chem. Sci.* 2025, **16**, 7239–7248.
79 J. Xue, Z. Qi, D. Yan, G. Yang, Y. Wang, *Angew. Chem. Int. Ed.* 2025, **64**, e202501951.

View Article Online
DOI: 10.1039/D5SC08423G

Data availability

No primary research results, software or code have been included and no new data were generated or analysed as part of this review.